



Universiteit  
Leiden  
The Netherlands

## **Multicenter in-house evaluation of an amplicon-based next-generation sequencing panel for comprehensive molecular profiling**

Jantus-Lewintre, E.; Rappa, A.; Ruano, D.; Egmond, D. van; Gallach, S.; Gozuyasli, D.; ... ; Barberis, M.

### **Citation**

Jantus-Lewintre, E., Rappa, A., Ruano, D., Egmond, D. van, Gallach, S., Gozuyasli, D., ... Barberis, M. (2025). Multicenter in-house evaluation of an amplicon-based next-generation sequencing panel for comprehensive molecular profiling. *Molecular Diagnosis & Therapy*, 29(2), 249-261. doi:10.1007/s40291-024-00766-2

Version: Publisher's Version

License: [Creative Commons CC BY-NC 4.0 license](https://creativecommons.org/licenses/by-nc/4.0/)

Downloaded from: <https://hdl.handle.net/1887/4299546>

**Note:** To cite this publication please use the final published version (if applicable).



# Multicenter In-House Evaluation of an Amplicon-Based Next-Generation Sequencing Panel for Comprehensive Molecular Profiling

Eloisa Jantus-Lewintre<sup>1</sup> · Alessandra Rappa<sup>2</sup> · Dina Ruano<sup>3</sup> · Demi van Egmond<sup>3</sup> · Sandra Gallach<sup>1</sup> · Dilce Gozuyasli<sup>4</sup> · Cecília Durães<sup>4</sup> · José Luis Costa<sup>4</sup> · Carlos Camps<sup>5</sup> · Ludovic Lacroix<sup>6</sup> · Karl Kashofer<sup>7</sup> · Tom van Wezel<sup>3,8</sup> · Massimo Barberis<sup>2</sup>

Accepted: 9 December 2024 / Published online: 11 January 2025  
© The Author(s) 2025

## Abstract

**Background** Predicting response to targeted cancer therapies increasingly relies on both simple and complex genetic biomarkers. Comprehensive genomic profiling using high-throughput assays must be evaluated for reproducibility and accuracy compared with existing methods.

**Methods** This study is a multicenter evaluation of the OncoPrint™ Comprehensive Assay Plus (OCA Plus) Pan-Cancer Research Panel for comprehensive genomic profiling of solid tumors. A series of 193 research samples (125 DNA and 68 RNA samples) was analyzed to evaluate the correlation and concordance of the OCA Plus panel with orthogonal methods, as well as its reproducibility ( $n = 5$  DNA samples) across laboratories.

**Results** The success rate for DNA and RNA sequencing was 96.6% and 89.7%, respectively. In a single workflow, the OCA Plus panel provided a detailed genomic profile with a high success rate for all biomarkers tested: single nucleotide variants/indels, copy number variants, and fusions, as well as complex biomarkers such as microsatellite instability, tumor mutational burden, and homologous recombination deficiency. The concordance for single nucleotide variants/indels was 94.8%, for copy number variants 96.5%, for fusions 94.2%, for microsatellite instability 80.8%, for tumor mutational burden 81.3%, and for homologous recombination deficiency 100%. The results showed high reproducibility across the five European research centers, each analyzing shared pre-characterized tissue biopsies (average of 1890 single nucleotide variants/indels per sample).

**Conclusions** This multicenter evaluation of the OCA Plus panel confirms the results of previous single-center studies and demonstrates the high reproducibility and accuracy of this assay.

## 1 Introduction

Many tumors harbor genetic alterations that can inform diagnosis, suggest disease prognosis, and guide treatment decisions. Next-generation sequencing (NGS) can help identify specific variants in tumor DNA that can be targeted with specific therapies [1, 2]. In addition, NGS enables the identification of co-mutations and new variants, further improving our understanding of the molecular foundations of cancer. Understanding the genetic profile of malignant solid tumors is therefore increasingly important to provide patients with cancer an optimal personalized treatment approach [3].

Actionable genetic alterations include single nucleotide variants (SNVs), small insertions and deletions (indels), fusions, splice variants, and copy number variants (CNVs),

including both gene amplifications and deletions [3]. Further information can be gained from complex biomarkers such as microsatellite instability (MSI) and tumor mutational burden (TMB), which affect the efficacy of immunotherapy [4, 5], and homologous recombination deficiency (HRD) status, which can predict sensitivity to targeted therapies in a range of cancers [6].

Comprehensive genomic profiling (CGP) can now assess hundreds of these clinically relevant cancer-related biomarkers in a single assay. This approach eliminates many of the challenges associated with sending samples to central laboratories for testing, as CGP assays can be integrated directly into clinical laboratory workflows. Further advantages of molecular profiling assays include a rapid turnaround time, the ability to screen a large number of genes without requiring specialized expertise, and large gene panels that can identify clinically relevant genetic variants in a single

Extended author information available on the last page of the article

### Key Points

This is a large (193 samples) multicenter evaluation of the OncoPrint™ Comprehensive Assay Plus panel for comprehensive genomic profiling in solid tumors.

The study demonstrates a high level of concordance and correlation with orthogonal testing, and high reproducibility of results when replicate samples were tested in different laboratories.

In a single workflow with a high level of automation and low material input, the OncoPrint™ Comprehensive Assay Plus panel provided a detailed genomic profile that included a wide range of single nucleotide variants, indels, copy number variants, fusions, as well as complex biomarkers such as microsatellite instability, tumor mutational burden, and homologous recombination deficiency status, in over 500 genes and multiple tumor types.

workflow [7, 8]. Given the inherent difficulty of obtaining biopsies from solid tumors, assays must also be able to work with small tissue samples that have low tumor cell content and/or yield low amounts of nucleic acids [9]. Any new sequencing technology must address all of these issues and generate data comparable to reference sequencing methods to ensure reliability and consistent results.

The OncoPrint™ Comprehensive Assay Plus panel (OCA Plus; Thermo Fisher Scientific, Waltham, MA, USA) is capable of detecting a variety of single- and multiple-gene biomarkers in over 500 cancer-associated genes. The performance of the OCA Plus panel has been evaluated in comparison to orthogonal methods [10, 11]. However, such single-center studies were not designed to demonstrate the reproducibility of the assay in different settings.

Here, we describe the largest evaluation study of the OCA Plus panel, which was conducted in five centers across Europe and examined a wide range of research tumor types. The OCA Plus panel was used to detect key simple (SNV/indels, CNV, fusions) and complex (TMB, MSI, HRD status) biomarkers in formalin-fixed paraffin-embedded (FFPE) samples from tumor biopsies. The samples pre-characterized with orthogonal methods were tested with the OCA Plus panel, and the results were compared to assess correlation and concordance. The reproducibility of the assay was evaluated using a series of five unique samples exchanged between the five participating laboratories. This study is the largest to investigate the use of the OCA Plus panel for CGP in a cohort of research pan-cancer samples.

## 2 Materials and Methods

### 2.1 Study Centers and Sample Selection

The multicenter evaluation was conducted in five laboratories at academic and clinical research centers around Europe: Medical University of Graz, Graz, Austria (laboratory 1); Leiden University Medical Center, Leiden, The Netherlands (laboratory 2); Istituto Europeo di Oncologia, Milan, Italy (laboratory 3); Institut Gustave Roussy, Paris, France (laboratory 4); and Fundación Investigación Hospital General Universitario, València, Spain (laboratory 5). A total of 193 research FFPE tissue samples were analyzed, with each center selecting samples from its own biobank material (Table S1a of the Electronic Supplementary Material [ESM]). Formalin-fixed paraffin-embedded samples were eligible for analysis if they had a minimum tumor cell content of 10% determined by local pathologists and a confirmed relevant genetic alteration determined by a validated orthogonal method. Most FFPE samples (96.5%) were  $\leq 5$  years old (2017–22) when nucleic acids were isolated for orthogonal testing, with additional isolation and OCA Plus panel testing conducted in 2022. Several orthogonal methods were included, namely NGS, fluorescence in situ hybridization, real-time polymerase chain reaction, and methylation assays. A complete list is available in Table S1a of the ESM. This study was approved by the institutional review boards of the five research centers.

### 2.2 Assay Pre-Assessment and Evaluation Phases 1 and 2

Prior to the evaluation phase of this study, centers 1, 3, and 5 pre-assessed the laboratory conditions and assay performance using two commercially available synthetic control samples, HD789 (Structural Multiplex FFPE DNA Reference Standard) and HD827 (OncoSpan gDNA Multiplex) from Horizon (Horizon Discovery, Waterbeach, UK; Tables S1b, c of the ESM).

In the evaluation phases 1 and 2, the OCA Plus panel was used to examine relevant genetic biomarkers. In phase 1, each center analyzed samples previously characterized by orthogonal methods and known to harbor one or more of the genomic variants. Each center selected a set of DNA samples that were analyzed for five biomarker types (SNV/indels, CNVs, MSI, TMB, and HRD), using the OCA Plus panel resulting in a total of 125 unique DNA samples. Another set of 68 RNA samples, also selected by each center, was used to examine gene fusions.

In phase 2, each center sent a DNA sample to all other centers to test for each biomarker type: laboratory 1 provided a sample for HRD analysis, laboratory 2 for MSI,

laboratory 3 for TMB, laboratory 4 for CNVs, and laboratory 5 for SNVs/indels. In this phase, five unique samples were exchanged among five laboratories, sequenced and analyzed to determine the reproducibility of the assay.

### 2.3 Nucleic Acid Isolation

Extraction of nucleic acids from research FFPE samples was performed using the methods listed in Table S1a of the ESM and according to the manufacturer's instructions.

### 2.4 Genomic Profiling by NGS

The OCA Plus panel covers 501 cancer-associated genes over 1.4 Mb of coding sequence, including 49 driver genes in over 1300 different fusions and splice-site variants, identified from RNA-paired samples. The libraries were prepared manually according to the protocol for the OCA Plus panel and templated with the Ion Chef™ System. A total of 20 ng of DNA was treated with uracil DNA glycosylase (Thermo Fisher Scientific) to remove deaminated cytosines that would cause a non-biologically relevant C > T transition. Complementary DNA was synthesized from 20 ng of RNA using the Ion Torrent™ NGS Reverse Transcription Kit (Thermo Fisher Scientific). Sequencing was performed using Ion 550™ chips on the Ion GeneStudio™ S5 Plus System with Torrent Suite version 5.16 (Thermo Fisher Scientific). Data were automatically transferred to Ion Reporter™ 5.20 (IR5.20; Thermo Fisher Scientific). Variants were called and annotated with OncoPrint Comprehensive Plus-w3.1 workflow in IR5.20, using human genome assembly 19 (HG19; GRCh37). The OncoPrint Comprehensive Plus Workflow in IR automates the calculation of tumor cell content (% of tumor cells) by analyzing genomic ploidy levels using heterozygous population SNPs and copy number ratios through the CNV pipeline. If the automated calculation is unavailable, pathologist-determined values can be manually entered for processing.

The TMB score is calculated by dividing the total number of exonic non-synonymous somatic mutations (i.e., missense and nonsense SNVs, frameshift and non-frameshift indels) by the total number of bases covered at least 60×. Somatic mutations are determined by the TMB filter chain, which filters in mutations with an allele fraction  $\geq 5\%$  and filters out germline variants using population databases of the 1000 Genomes Project, NHLBI GO Exome Sequencing Project, Single Nucleotide Polymorphism Database, and Exome Aggregation Consortium. A TMB score threshold of ten or more mutations/Mb was used to classify TMB status as high or low. The MSI score

is calculated considering 76 microsatellite loci known to be affected by MSI. The Ion Reporter software compares the signal of the targeted microsatellites from the tumor sample with that of an in-sample standard (RMC) to calculate an MSI score. A sample is classified MSI-high if the MSI score is higher than a predetermined threshold. Microsatellite instability status was categorized as high if the score was  $\geq 19$ . The OCA Plus panel calculates the genomic instability metric (GIM), a proprietary measurement in Ion Reporter Software that quantifies genomic scarring associated with HRD. It summarizes unbalanced copy number changes in autosomes determined using genomic segmentation and generates a value between 0 and 100. The higher the value, the more genomic instability (GI) is observed in the sample. Homologous recombination deficiency status (positive or negative) was determined using a combined approach comprising *BRCA1/2* mutation status and the GIM threshold established for ovarian cancer ( $\geq 16 = \text{GI-high}$ ,  $< 16 = \text{GI-low}$ ). Copy number variant estimates were made by counting the reads for each amplicon compared with the expected reads for those amplicons in a "normal" sample. The limit of detection (LOD) of the copy number was estimated by an algorithm trained on many different samples to capture systematic effects. This algorithm established the LOD for copy number gain as 6 and copy number loss as a 0.5-fold difference.

The success of DNA and RNA sequencing was assessed using the following performance indicators: total mapped reads, mean coverage, mean absolute pairwise distance, number of amplicons above 500×, number of amplicons above 250×, and mean read length. The quality control (QC) criteria for successful DNA sequencing were > 22 million total mapped reads, mean coverage > 800×, and mean absolute pairwise distance < 0.5, while successful RNA sequencing required > 500 K total mapped reads.

### 2.5 Data Analysis

The analytical evaluation included measurements of correlation, concordance, and reproducibility of the results from the OCA Plus panel in the five centers compared with the previously used standard orthogonal methods. The correlation between biomarkers was assessed by calculating the R-squared ( $R^2$ ) or Pearson correlation coefficients. Data analysis and visualization were performed using R (version 4.2.2), Microsoft Office Excel (version 2309; Microsoft Corporation, Redmond WA, USA), and GraphPad Prism (version 10.1.0; GraphPad Software, Boston, MA, USA).

### 3 Results

#### 3.1 Sample Characterization

The FFPE research samples used for the analytical evaluation of the OCA Plus panel included a range of tumor types (Fig. S1a and Table S1a of the ESM). A total of 125 samples were used for DNA sequencing. The most common tumor types included lung ( $n = 34$ ), colorectal ( $n = 18$ ), ovarian ( $n = 16$ ), skin ( $n = 11$ ), and endometrial ( $n = 11$ ) cancers, as well as central nervous system tumors ( $n = 7$ ), cancer of unknown primary ( $n = 6$ ), and breast cancer ( $n = 5$ ). Sixty-eight samples were submitted for RNA sequencing, including lung cancer ( $n = 47$ ), thyroid cancer ( $n = 6$ ), skin cancer ( $n = 3$ ), central nervous system tumor ( $n = 2$ ), breast cancer ( $n = 2$ ), hematologic neoplasms ( $n = 2$ ), and other solid tumors ( $n = 6$ ).

The tumor cell content in the tissue samples was successfully calculated using the OCA Plus software in 94.4% of samples and ranged from 10 to 100% (Fig. S1b of the ESM). All samples tested harbored at least one of the genomic variants under investigation in this study.

#### 3.2 Evaluation Using Commercial Control Samples

The performance of the OCA Plus panel was pre-evaluated in three centers using two commercially available control samples. This showed an average concordance of 98.1% with the expected values (Table S2 of the ESM). The parameters observed in these three laboratories were in line with the expected values, including allele fractions, number of variants detected, and copy numbers (Fig. S2a–e of the ESM). The *MET* amplification expected in the control sample HD789 was below the LOD of this assay (Fig. S2e of the ESM).

#### 3.3 Sequencing Success Criteria and OCA Plus Panel Performance Indicators

The success of the DNA and RNA sequencing runs was assessed using a set of assay performance indicators and QC criteria (Fig. S3a–g of the ESM). Of the 145 DNA samples sequenced at the five centers (125 unique samples selected plus one sample from each laboratory shared with the other four), 140 met the predetermined criteria, corresponding to an overall success rate of 96.6%. A total of 61 RNA samples met the specified QC criteria, corresponding to a success rate of 89.7%. The overall success rate for sequencing both DNA and RNA with the OCA Plus panel was 93.9%.

#### 3.4 Detection of Simple Biomarkers: SNVs, Indels, CNVs, and Fusions

##### 3.4.1 SNV/Indels

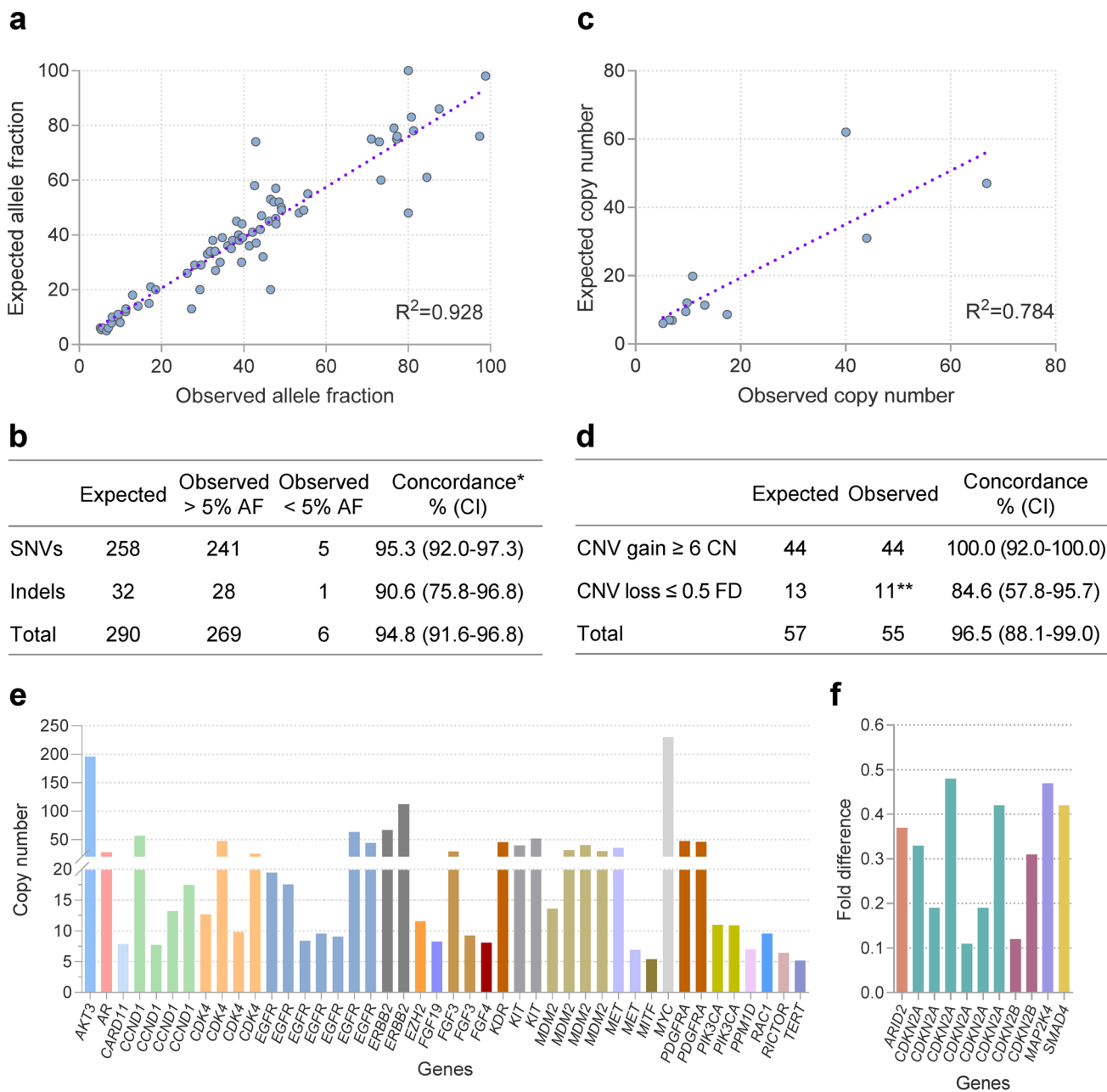
Overall, there was a good correlation between the results obtained with the OCA Plus panel and the orthogonal methods for the SNVs/indels allele fractions ( $R^2 = 0.928$ ) (Fig. 1a). Detailed information on allele fraction and the number of variants per gene in the DNA samples is provided in Fig. S4 of the ESM. There was a high concordance (94.8%) with the expected SNVs and indels (Fig. 1b). Of the 275 SNVs/indels detected, six concordant variants were identified despite being below the LOD (<5% allele fraction).

##### 3.4.2 CNVs

There was a good correlation between the results of the OCA Plus panel and orthogonal methods for CNV copy number ( $R^2 = 0.784$ ) (Fig. 1c). The overall concordance for CNVs across the set of 37 samples was also high (96.5%) (Fig. 1d). The OCA Plus panel is capable of detecting both gene amplifications and deletions. Most of the CNVs detected were amplifications (defined as a gain of  $\geq 6$  copy number), which were 100% concordant with expected values. Forty-four gene amplifications were observed in 22 genes, including *EGFR*, *CDK4*, *CCND1*, and *MDM2* (Fig. 1e of the ESM). Concordance was lower for CNV losses (defined as a  $\leq 0.5$ -fold difference, 84.9%), and these were observed in five genes, including *CDKN2A* and *CDKN2B* (Fig. 1f).

##### 3.4.3 Gene Fusions and Splice-Site Variants

A total of 49 out of 52 expected targeted fusions with driver genes (such as *ALK*, *RET*, *FGFR3*, *NTRK3*, Fig. S5a, b of the ESM) and *MET* exon 14 skipping variants were verified with the OCA Plus panel, with 94.2% concordance (Fig. 2a). In addition, novel fusions were detected in three out of five cases by an exon tiling imbalance (Fig. 2a and Fig. S5c, d of the ESM). Two expected novel fusions were not detected with an exon tiling imbalance because of low expression levels and insufficient reads per driver gene. A total of 22 distinct gene fusions were detected, including fusions with the known oncogenes *ALK*, *RET*, *ROS1*, *NTRK1* and 3, and *FGFR3*; detailed information is provided in Fig. 2b. The fusions *EML4::ALK*, *KIF5B::RET*, and *MET* exon 14 skipping variants were detected in a high proportion (Fig. 2b).

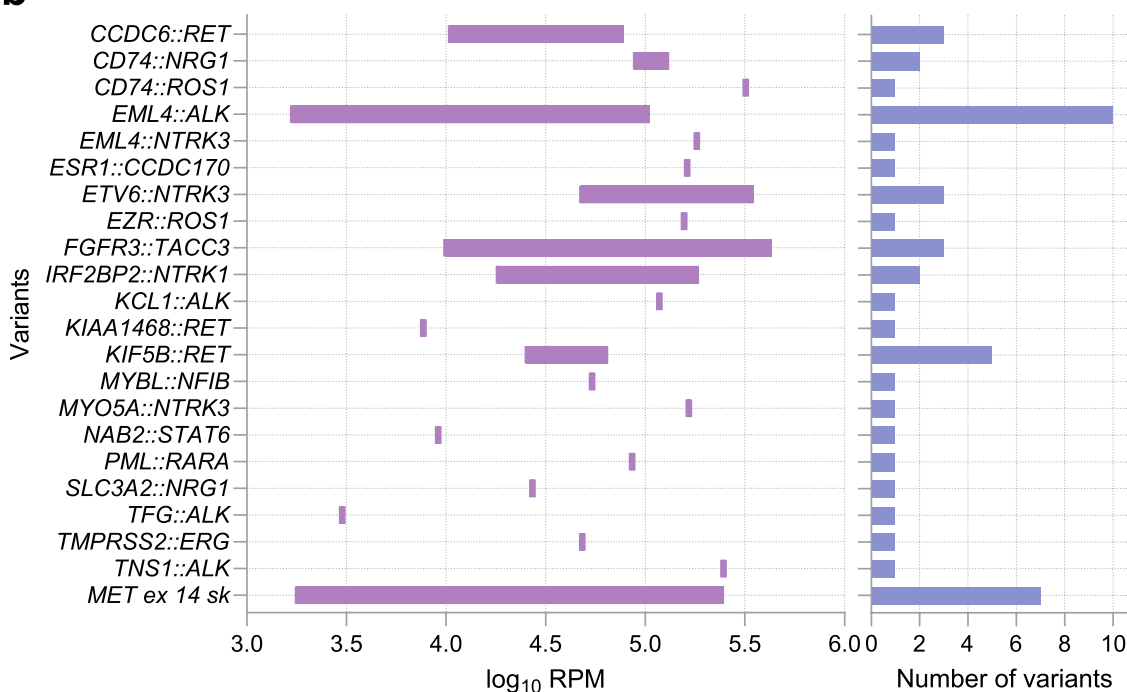


**Fig. 1** Detection of single nucleotide variants/insertions or deletions (SNVs/indels) and copy number variants (CNVs) by the OCA Plus panel. **(a)** Correlation of the SNVs/indels allele fraction (AF). **(b)** Correlation of CNVs. **(c)** Concordance (shown as % with 95% confidence interval [CI]) determined for SNVs and indels. Numbers in the table represent the number of samples tested. \*Concordance was calculated irrespective of the 5% AF limit. **(d)** Concordance (shown as % with 95% CI) determined for CNVs. Numbers in the table repre-

sent the number of samples tested. \*\*One expected *RB1* copy number (CN) deletion was detected above the threshold and thereby counted as a false negative. **(e)** Detection of gene amplifications (defined as a gain of  $\geq 6$  CN), which showed 100% concordance with expected values. **(f)** Detection of gene deletions (defined as a  $\leq 0.5$ -fold difference [FD]). Each gene is represented by a uniquely colored bar, with each bar indicating a specific CN or FD value

**a**

Targeted variants			Novel variants		
OCA Plus			OCA Plus		
Orthogonal method	Positive	Negative	Orthogonal method	Positive	Negative
Positive	49	2	Positive	3	2
Negative	1	0	Negative	1	0
Concordance (% , CI)	94.2 (84.4-98.0)		Concordance (% , CI)	50.0 (18.8-81.2)	

**b**

**Fig. 2** Detection of gene fusions in RNA research samples with the OCA Plus panel. **(a)** Concordance (shown as % with 95% confidence interval [CI]) determined for variants expected in RNA samples (gene fusions and *MET* exon 14 skipping). Numbers in the table represent

the number of samples tested. Fusion limit of detection (LOD) taken as >1000 read counts per million. **(b)** Gene fusions shown as read counts per million ( $\log_{10}$  RPM), and number of fusions and *MET* exon 14 skipping (*MET* ex 14 sk) variants

### 3.5 Detection of Complex Biomarkers: MSI, TMB, and HRD Status

#### 3.5.1 MSI

The MSI success rate was 95.7%, with 134 of 140 sequenced samples meeting the QC criteria to obtain an MSI score. The concordance of MSI status was calculated in the 26 samples previously characterized by orthogonal methods

(Fig. 3). The samples comprised eight tumor types, including colorectal (all MSI-high) and endometrial (all MSI-low, as determined by the OCA Plus panel). Five of the 26 samples were identified as MSI-high by orthogonal testing but MSI-low by the OCA Plus panel (Table S3 of the ESM). These discordant samples were either endometrial cancer or cholangiocarcinoma. The overall concordance with orthogonal testing for MSI status was 80.8%.

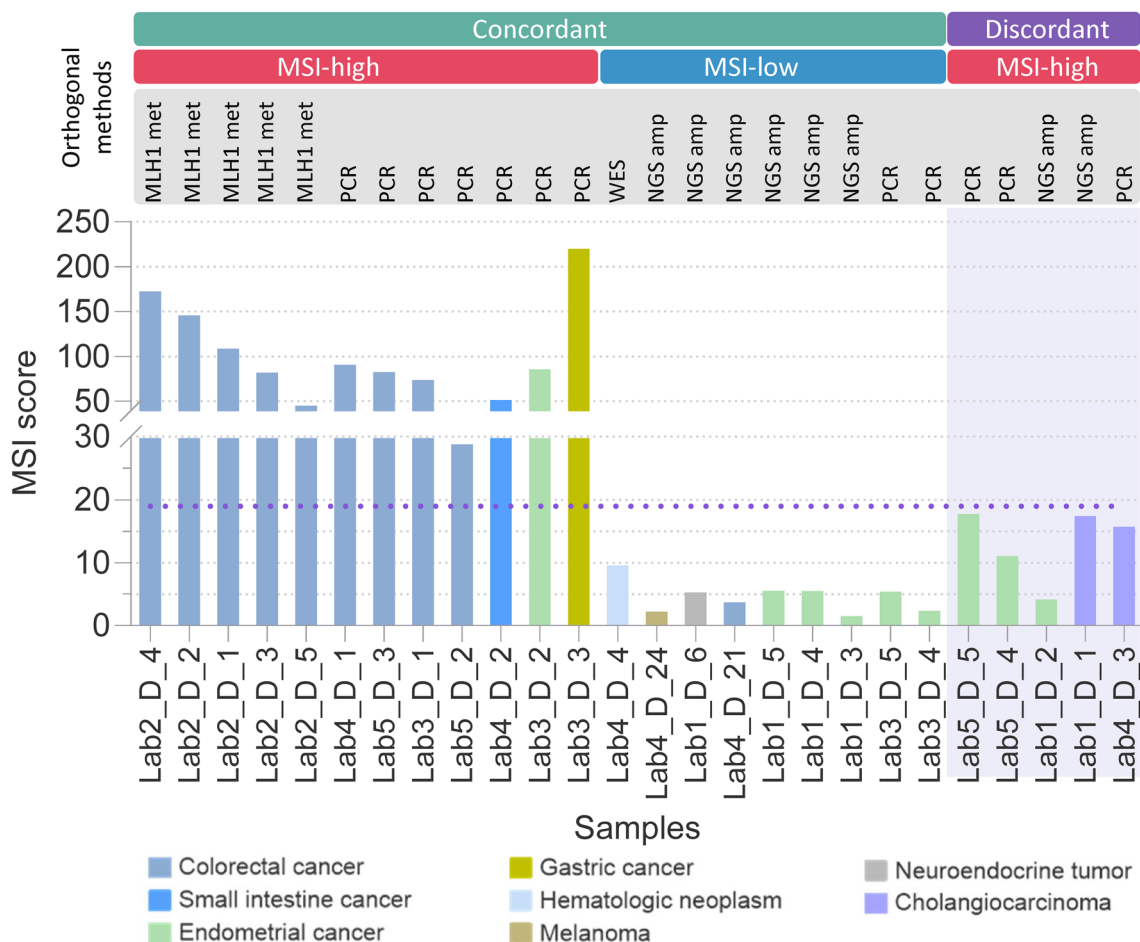


**Fig. 3** Evaluation of microsatellite instability (MSI) status in different types of cancer samples using the OCA Plus panel. MSI status was pre-determined using various orthogonal methods (top horizontal bars). The dotted line indicates the MSI score threshold ( $\geq 19 =$  MSI-high). The shaded area indicates discordant samples identified

as MSI-high by orthogonal methods but not identified as MSI-high by the OCA Plus panel. *lab* laboratory, *MLH1 met* *MLH1* promoter methylation detection method, *NGS amp* NGS amplicon-based method, *WES* whole exome sequencing (RNAseq)

### 3.5.2 TMB

The TMB score was successfully calculated in 100% of the 140 samples sequenced. The correlation between the TMB scores calculated with the OCA Plus panel and the orthogonal methods was high ( $R^2 = 0.794$ , Fig. 4a). Concordance with the orthogonal tests was 81.3% (Table S4 of the ESM), with disagreement on TMB status in only six of the 32 samples. These discordant samples are shown in Fig. 4b, along with the details of the orthogonal testing method used to characterize each sample, tumor type, and TMB status. As deamination effects can contribute to altered TMB scores, the OCA Plus panel calculates a deamination score to aid interpretation in borderline or discordant cases (Fig. 4b). Mutations in the exonuclease domains of DNA polymerase  $\epsilon$  (*POLE*) and/or DNA polymerase  $\delta$  (*POLD1*) were detected in four samples, all of which were TMB-high.

### 3.5.3 HRD

Homologous recombination deficiency status in ovarian cancer samples was determined by incorporating *BRCA1/2* mutation status and GIM. The GIM threshold established for ovarian cancer ( $\geq 16 =$  GI-high,  $< 16 =$  GI-low) was empirically applied to obtain an HRD status for breast cancer samples, as there is no established HRD threshold for breast cancer. The GIM was calculated in 94.2% of sequenced samples that met the QC criteria (132 of 140 samples). Eighteen samples ( $n = 13$  ovarian cancer,  $n = 5$  breast cancer) were pre-characterized by orthogonal methods (Fig. 5). The combined approach to determine HRD status, where the presence of a *BRCA1/2* variant and/or high GI status indicates HRD positive, was 100% concordant with results obtained by orthogonal methods (Table S5 of the ESM).



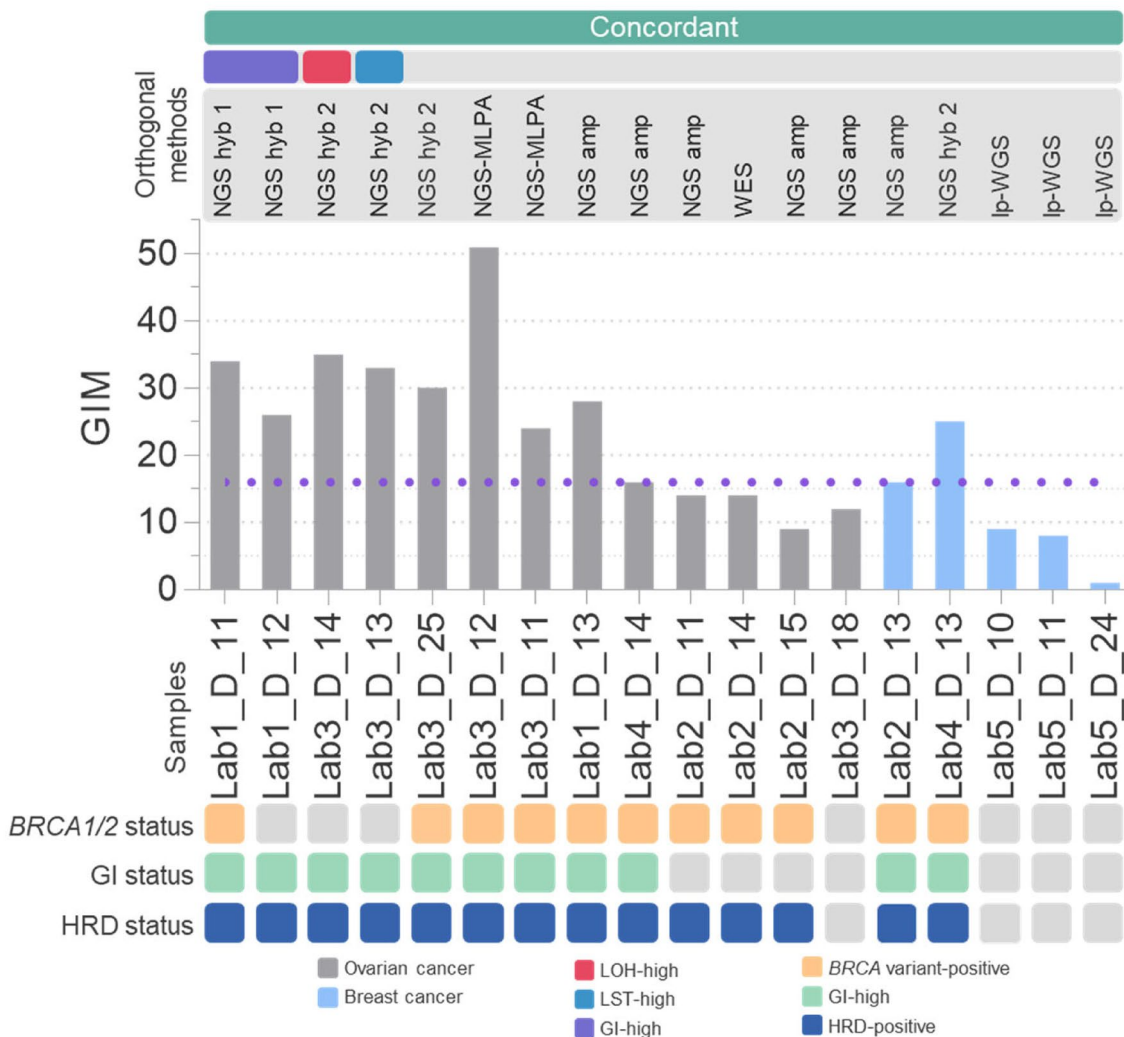


**Fig. 5** Evaluation of homologous recombination deficiency (HRD) in ovarian and breast cancer samples using the OCA Plus panel. HRD status was pre-determined using different orthogonal methods (top bars). Genomic instability (GI) in the OCA Plus panel was determined using the genomic instability metric. *BRCA1/2* mutation status as determined by OCA Plus is represented to provide additional information on HRD status. The dotted line indicates the genomic

instability metric score threshold ( $\geq 16 = \text{GI-high}$ ,  $< 16 = \text{GI-low}$ ). *lab* laboratory, *LOH* loss of heterozygosity, *lp-WGS* low-pass whole genome sequencing, *LST* large-scale state transitions, *MLPA* multiplex ligation-dependent probe amplification method, *NGS amp* NGS amplicon-based method, *NGS hyb 1* NGS hybrid capture method 1, *NGS hyb 2* NGS hybrid capture method 2, *WES* whole exome sequencing (RNAseq)

### 3.6 Evaluation of the OCA Plus Panel Reproducibility

Data from phase 2 of the evaluation study (Table 1) showed a high level of reproducibility with the OCA Plus panel, with 88.2% (1940) to 95.4% (1844) of SNVs/indels (allele fraction  $> 5\%$ ) detected in all replicate DNA samples assayed at the five centers. The percentage of unique SNVs/indels (allele fraction  $> 5\%$ ) detected by one, two, three, or four laboratories was very low, with a range from 0.7% (13–15) to 6.6% (144), depending on the sample analyzed. Each of the five laboratories evaluated an average of 1890 SNVs/indels per sample. The median reproducibility of SNV/indel

detection with the OCA Plus panel reached 94.0% overall, as shown by the median correlation of allele fraction for samples shared between laboratories (calculated using Pearson correlation, Fig. S6a of the ESM).

Testing conducted with the OCA Plus panel on replicate samples in all five study laboratories also showed consistency for complex biomarkers. The same MSI status was determined for all five samples in all centers, with only minor variations in absolute MSI scores (Fig. S6b of the ESM). Regarding TMB status, the results in all five centers were in agreement for four of the five samples, while the absolute TMB scores for the replicates of the fifth sample

**Table 1** Number of SNVs/indels detected per lab in replicate DNA samples during phase II of the study used to evaluate the reproducibility of the OCA Plus panel

Sample	All SNVs/indels <i>n</i> (%)	Unique SNVs/indels <i>n</i> (%)			
		4 labs	3 labs	2 labs	1 lab
Lab1_D_12	1828 (93.3)	26 (1.3)	17 (0.9)	17 (0.9)	71 (3.6)
Lab2_D_4	1940 (88.2)	68 (3.1)	20 (0.9)	27 (1.2)	144 (6.6)
Lab3_D_7	1950 (93.8)	24 (1.2)	16 (0.8)	15 (0.7)	73 (3.5)
Lab4_D_16	1889 (92.6)	38 (1.9)	18 (0.9)	23 (1.1)	71 (3.5)
Lab5_D_21	1844 (95.4)	33 (1.7)	13 (0.7)	13 (0.7)	31 (1.6)

*lab* laboratory, *SNVs* single nucleotide variants

(Lab3\_D\_7) were higher (laboratories 3 and 4) or lower than the TMB threshold (Fig. S6c of the ESM).

The reproducibility of GIM was tested on all replicate samples regardless of tumor type. The tests performed in the five laboratories showed consistent GIM results with minor variations possibly related to the performance of the samples between replicates (e.g., MAPD variability, Fig. S6d of the ESM).

## 4 Discussion

This pan-cancer study represents a large, multicenter, analytical performance evaluation of the OCA Plus panel. The methodology provides a robust molecular testing assessment and demonstrates high concordance between the OCA Plus panel and orthogonal reference methods, as well as high reproducibility, a high rate of successful sequencing runs, and efficacy using FFPE research samples from a wide range of tumor types. The OCA Plus panel detected many genetic alterations classified as high-tier molecular targets [3].

The OCA Plus panel showed a high correlation with orthogonal methods in the detection of biomarkers such as SNVs, indels, CNVs, splice variants, and fusions. The high number of SNVs/indels detected in the samples resulted in an excellent correlation of allele fractions ( $R^2 = 0.928$ ). For CNVs, the correlation of copy numbers was strongest at low copy numbers (<20), yet the presence of three CNVs at higher copy numbers diluted the overall correlation with orthogonal methods ( $R^2 = 0.784$ ).

In addition, the OCA Plus panel detected 49 of the expected variants in the RNA samples at the five centers, including known gene fusions and *MET* exon 14 skipping. These variants included oncogenic gene fusions of the *NTRK* gene that are present in various tumor types and have emerged as targets for cancer-agnostic therapies in *NTRK* fusion-positive solid tumors [12–14]. Other fusions detected include *RET*, *FGFR1-3*, and *ALK*. The OCA Plus panel may help address the practical challenges of detecting

gene fusions in decentralized laboratories [15, 16], while also providing insights into the genetic basis of cancer that could serve as a focus for future research.

Comprehensive genomic testing that detects complex biomarkers such as MSI, TMB, and HRD provides further information for clinical outcomes, but is hampered by technological complexity [17]. Both MSI and TMB are predictive biomarkers of response to immunotherapy [4, 5], and therefore the clinical utility of these complex biomarkers is increasing. The growing need to assess MSI and TMB in the clinical setting prompted the ESMO to develop consensus recommendations on appropriate testing methods. The expert panel concluded that the ability to assess both MSI and TMB in single-gene panels makes NGS an important tool for the selection of patients for immunotherapy [4].

Microsatellite instability is a marker for tumors caused by defective DNA mismatch repair. Analysis of MSI status is particularly important in several tumor types, including intestinal (colorectal and small bowel), endometrial, gastric, esophageal, ovarian, and glioblastoma, and can be targeted with approved immunotherapy [18, 19]. Microsatellite instability status was reliably determined with the OCA Plus panel in most of these tumor types, with high concordance with orthogonal assays, including 100% concordance in colorectal tumor samples. Discordances between the MSI status determined by the OCA Plus panel and orthogonal methods include three endometrial tumors and two cholangiocarcinomas with MSI scores near the predetermined OCA Plus threshold. While the threshold for defining categories for MSI status in colorectal cancer is well established, this has not been verified for endometrial cancer. Determining the optimal threshold for defining MSI categories from NGS data of endometrial tumor samples is not straightforward and is a matter of ongoing debate in the scientific community [20, 21].

Tumor mutational burden reflects the number of exonic non-synonymous somatic mutations in the genome of a tumor. A high TMB score indicates a high likelihood of neoantigen formation and thus serves as a predictive biomarker

for the response to immunotherapy [22]. The OCA Plus panel was able to measure the TMB score in all sequenced samples covering multiple tumor types, with 81.3% concordance with orthogonal methods. As in the case of MSI, the six discordant samples exhibit TMB scores close to the threshold that defines the TMB-low and TMB-high categories, thus slight variations may change the classification of TMB status. The discordant samples were pre-characterized by whole genome sequencing or targeted hybrid capture-based NGS. Some degree of variability in estimating TMB between assays of different sizes is to be expected, particularly for samples with lower TMB [23]. Other factors contributing to this variability include tumor heterogeneity, sample handling, panel content, sequencing platforms, and bioinformatics pipelines [17, 23]. Moreover, deamination can occur in old or inadequately fixed FFPE samples [24], which can lead to false-positive TMB estimates. Four of the 32 samples analyzed for TMB concordance had conspicuously high TMB scores. All of them had *POLE* and/or *POLD1* gene mutations, which is consistent with the known association between high TMB and *POLE/POLD1* mutations [25, 26]. Other factors that have been associated with increased TMB are environmental factors, such as ultraviolet light in melanoma and smoking in lung cancer [27, 28].

In terms of complex biomarkers, some mutations are known to cause changes in proteins that cannot be directly targeted, but they affect cellular pathways that can be addressed. For example, mutations in the DNA homologous recombination repair pathway can be treated with drugs that inhibit the recognition of DNA damage by the PARP protein, regardless of which protein is affected. The OCA Plus panel covers 46 key genes in the homologous recombination repair pathway and measures genomic instability using the GIM. Defects in the homologous recombination repair pathway, such as loss-of-function or deleterious mutations in the associated genes, lead to higher levels of genomic instability and HRD. While the GIM threshold for ovarian cancer is well established, the threshold for breast cancer is not, and there is no consensus on the definition of the HRD status [6]. In this study, the OCA Plus panel showed 100% concordance with orthogonal HRD status in ovarian and breast tumors, regardless of whether the different tumor types were analyzed together under the same GIM threshold.

The OCA Plus panel is combined with the ability to detect a wide range of mutations and complex biomarkers in a single workflow. The capacity to routinely analyze processed FFPE tumor samples without the need for specialized sample preparation and large amounts of tissue is clearly advantageous. The present evaluation was performed with FFPE research samples already stored in the biobank of each academic or clinical research center, each with different amounts and sources of starting material as well as different proportions of neoplastic cells. The results showed

a high success rate in sequencing key biomarkers, even in samples with low tumor cell content. It has already been shown that the OCA Plus panel can detect more genetic changes compared with a high-throughput NGS platform, requires a lower DNA content in the samples, and library preparation is easier and takes less time [11]. The built-in automation of the OCA Plus workflow simplifies the variant analysis, providing a significant benefit. The complexities of a variant analysis and interpretation are key considerations for implementing CGP in the laboratory and standardizing genomic insights [29].

In addition to the present study, the performance of the OCA Plus panel for CGP has been evaluated in research studies in various advanced solid tumor types, including the detection of mutations in genes of the homologous recombination pathway, the estimation of LOH and TMB [30–32]. This suggests that the OCA Plus panel could streamline such analysis in processed FFPE tumor samples in the future, eliminating the need for special sample preparation. It could also facilitate the analysis of large cohorts of samples with CGP sequencing and assist pathologists in evaluating tissue samples through decentralized testing [9]. In summary, the OCA Plus panel has demonstrated high analytical performance in the detection of simple and complex biomarkers, highlighting it as a platform for CGP in a wide range of tumor types.

## 5 Conclusions

This evaluation study demonstrates that the OCA Plus panel consistently detects relevant genetic alterations in research FFPE samples. With the capacity to detect alterations in more than 500 genes in a single streamlined process, the OCA Plus panel is a valuable tool for CGP in oncology research.

**Supplementary Information** The online version contains supplementary material available at <https://doi.org/10.1007/s40291-024-00766-2>.

**Acknowledgements** The authors thank Mafalda Ramos de Matos (Thermo Fisher Scientific) for assistance with the data and manuscript review and Lieneke Steeghs, Anne-Marie Cleton Jansen (Leiden University Medical Center), and Linda Bosch (Netherlands Cancer Institute/AVL) for providing samples and assistance with the data analysis. Scientific Writers Ltd., Edinburgh, UK supported the manuscript writing.

## Declarations

**Funding** This study was supported in part by Thermo Fisher Scientific in the form of reagents. The content is solely the responsibility of the authors.

**Conflict of interest** Dilce Gozuyasli, Cecília Durães, and José Luis Costa are employees of Thermo Fisher Scientific. Eloisa Jantus-

Lewintre, Alessandra Rappa, Dina Ruano, Demi van Egmond, Sandra Gallach, Carlos Camps, Ludovic Lacroix, Karl Kashofer, Tom van Wezel, and Massimo Barberis have no conflicts of interest that are directly relevant to the content of this article.

**Ethics approval** This retrospective study was based on pre-existing biological materials and data, which were reanalyzed using a new method. All procedures were conducted in accordance with the ethical standards outlined by the relevant institutional and/or national research committees and adhered to the principles of the Helsinki Declaration (revised in 2013). The study received approval from the following ethics committees: Medical University of Graz (33-112 ex 20/21), Istituto Europeo di Oncologia (IEO DSC.MO.7720), Leiden University Medical Center (following the Code Proper Secondary Use of Human Tissue established by the Dutch Federation of Medical Sciences, <https://www.federa.org/>), Institut Gustave Roussy (s/n), Fundación Investigación Hospital General Universitario (s/n).

**Consent to participate** Written informed consent was obtained from all patients to use their biological samples for research purposes.

**Consent for publication** Not applicable.

**Availability of data and material** The datasets generated and/or analyzed during this study are available from the corresponding author upon reasonable request.

**Code availability** Not applicable.

**Author contributions** MB and JLC designed the study; EJ-L, CC, LL, KK, and TvW performed the data interpretation; AR, DR, DvE, and SG performed the experiments and data analysis; DG and CD performed the data analysis and visualization; EJL, CC, LL, KK, TvW, MB, DR, and DG revised the manuscript; CD and JLC reviewed and edited the manuscript. All authors have read and agreed to the final version of the manuscript.

**Open Access** This article is licensed under a Creative Commons Attribution-NonCommercial 4.0 International License, which permits any non-commercial use, sharing, adaptation, distribution and reproduction in any medium or format, as long as you give appropriate credit to the original author(s) and the source, provide a link to the Creative Commons licence, and indicate if changes were made. The images or other third party material in this article are included in the article's Creative Commons licence, unless indicated otherwise in a credit line to the material. If material is not included in the article's Creative Commons licence and your intended use is not permitted by statutory regulation or exceeds the permitted use, you will need to obtain permission directly from the copyright holder. To view a copy of this licence, visit <http://creativecommons.org/licenses/by-nc/4.0/>.

## References

- Sicklick JK, Kato S, Okamura R, Schwaederle M, Hahn ME, Williams CB, et al. Molecular profiling of cancer patients enables personalized combination therapy: the I-PREDICT study. *Nat Med.* 2019;25(5):744–50.
- Ozdogan M, Papadopoulou E, Tsoulos N, Tsantikidi A, Mariatou VM, Tsaousis G, et al. Comprehensive tumor molecular profile analysis in clinical practice. *BMC Med Genom.* 2021;14(1):105.
- Mateo J, Chakravarty D, Dienstmann R, Jezdic S, Gonzalez-Perez A, Lopez-Bigas N, et al. A framework to rank genomic alterations as targets for cancer precision medicine: the ESMO Scale for Clinical Actionability of molecular Targets (ESCAT). *Ann Oncol.* 2018;29(9):1895–902.
- Luchini C, Bibeau F, Ligtenberg MJL, Singh N, Nottegar A, Bosse T, et al. ESMO recommendations on microsatellite instability testing for immunotherapy in cancer, and its relationship with PD-1/PD-L1 expression and tumour mutational burden: a systematic review-based approach. *Ann Oncol.* 2019;30(8):1232–43.
- Palmeri M, Mehnert J, Silk AW, Jabbour SK, Ganesan S, Popli P, et al. Real-world application of tumor mutational burden-high (TMB-high) and microsatellite instability (MSI) confirms their utility as immunotherapy biomarkers. *ESMO Open.* 2022;7(1):100336.
- Stewart MD, Merino Vega D, Arend RC, Baden JF, Barbash O, Beaubier N, et al. Homologous recombination deficiency: concepts, definitions, and assays. *Oncologist.* 2022;27(3):167–74.
- Marchio C, Scaltriti M, Ladanyi M, Iafrate AJ, Bibeau F, Dietel M, et al. ESMO recommendations on the standard methods to detect NTRK fusions in daily practice and clinical research. *Ann Oncol.* 2019;30(9):1417–27.
- Imyanitov EN, Iyevleva AG, Levchenko EV. Molecular testing and targeted therapy for non-small cell lung cancer: current status and perspectives. *Crit Rev Oncol Hematol.* 2021;157: 103194.
- Mathieson W, Thomas GA. Why Formalin-fixed, Paraffin-embedded biospecimens must be used in genomic medicine: an evidence-based review and conclusion. *J Histochem Cytochem.* 2020;68(8):543–52.
- Vestergaard LK, Oliveira DNP, Poulsen TS, Hogdall CK, Hogdall EV. OncoPrint comprehensive assay v3 vs. oncoPrint comprehensive assay plus. *Cancers (Basel).* 2021;13(20):5230.
- Ottstad AL, Huang M, Emdad EF, Mjelle R, Skarpeteig V, Dai HY. Assessment of two commercial comprehensive gene panels for personalized cancer treatment. *J Pers Med.* 2022;13(1):42.
- Amatu A, Sartore-Bianchi A, Siena S. NTRK gene fusions as novel targets of cancer therapy across multiple tumour types. *ESMO Open.* 2016;1(2): e000023.
- Doebele RC, Drilon A, Paz-Ares L, Siena S, Shaw AT, Farago AF, et al. Entrectinib in patients with advanced or metastatic NTRK fusion-positive solid tumours: integrated analysis of three phase 1–2 trials. *Lancet Oncol.* 2020;21(2):271–82.
- Drilon A, Laetsch TW, Kummar S, DuBois SG, Lassen UN, Demetri GD, et al. Efficacy of larotrectinib in TRK fusion-positive cancers in adults and children. *N Engl J Med.* 2018;378(8):731–9.
- Belli C, Penault-Llorca F, Ladanyi M, Normanno N, Scoazec JY, Lacroix L, et al. ESMO recommendations on the standard methods to detect RET fusions and mutations in daily practice and clinical research. *Ann Oncol.* 2021;32(3):337–50.
- Nguyen MA, Colebatch AJ, Van Beek D, Tierney G, Gupta R, Cooper WA. NTRK fusions in solid tumours: what every pathologist needs to know. *Pathology.* 2023;55(5):596–609.
- Vega DM, Yee LM, McShane LM, Williams PM, Chen L, Vilimas T, et al. Aligning tumor mutational burden (TMB) quantification across diagnostic platforms: phase II of the Friends of Cancer Research TMB Harmonization Project. *Ann Oncol.* 2021;32(12):1626–36.
- Casak SJ, Marcus L, Fashoyin-Aje L, Mushti SL, Cheng J, Shen YL, et al. FDA approval summary: pembrolizumab for the first-line treatment of patients with MSI-H/dMMR advanced unresectable or metastatic colorectal carcinoma. *Clin Cancer Res.* 2021;27(17):4680–4.
- Marcus L, Lemery SJ, Keegan P, Pazdur R. FDA approval summary: pembrolizumab for the treatment of microsatellite instability-high solid tumors. *Clin Cancer Res.* 2019;25(13):3753–8.
- Wang Y, Shi C, Eisenberg R, Vnencak-Jones CL. Differences in microsatellite instability profiles between endometrioid and

- colorectal cancers: a potential cause for false-negative results? *J Mol Diagn.* 2017;19(1):57–64.
21. Wu X, Snir O, Rottmann D, Wong S, Buza N, Hui P. Minimal microsatellite shift in microsatellite instability high endometrial cancer: a significant pitfall in diagnostic interpretation. *Mod Pathol.* 2019;32(5):650–8.
  22. Marcus L, Fashoyin-Aje LA, Donoghue M, Yuan M, Rodriguez L, Gallagher PS, et al. FDA approval summary: pembrolizumab for the treatment of tumor mutational burden-high solid tumors. *Clin Cancer Res.* 2021;27(17):4685–9.
  23. Buttner R, Longshore JW, Lopez-Rios F, Merkelbach-Bruse S, Normanno N, Rouleau E, et al. Implementing TMB measurement in clinical practice: considerations on assay requirements. *ESMO Open.* 2019;4(1): e000442.
  24. Kim S, Park C, Ji Y, Kim DG, Bae H, van Vrancken M, et al. Deamination effects in formalin-fixed, paraffin-embedded tissue samples in the era of precision medicine. *J Mol Diagn.* 2017;19(1):137–46.
  25. Huhns M, Nurnberg S, Kandashwamy KK, Maletzki C, Bauer P, Prall F. High mutational burden in colorectal carcinomas with monoallelic POLE mutations: absence of allelic loss and gene promoter methylation. *Mod Pathol.* 2020;33(6):1220–31.
  26. Ma X, Dong L, Liu X, Ou K, Yang L. POLE/POLD1 mutation and tumor immunotherapy. *J Exp Clin Cancer Res.* 2022;41(1):216.
  27. Jardim DL, Goodman A, de Melo GD, Kurzrock R. The challenges of tumor mutational burden as an immunotherapy biomarker. *Cancer Cell.* 2021;39(2):154–73.
  28. Wang X, Ricciuti B, Nguyen T, Li X, Rabin MS, Awad MM, et al. Association between smoking history and tumor mutation burden in advanced non-small cell lung cancer. *Cancer Res.* 2021;81(9):2566–73.
  29. Adams HP, Hiemenz MC, Hertel K, Fuhlbruck F, Thomas M, Oughton J, et al. Comparison of results from two commercially available in-house tissue-based comprehensive genomic profiling solutions: research use only AVENIO Tumor Tissue Comprehensive Genomic Profiling Kit and TruSight Oncology 500 Assay. *J Mol Diagn.* 2024;26(11):1018–33.
  30. Mesquita A, Ferro A, Machado JC, Schmitt F. Next-generation sequencing of breast cancer in the neoadjuvant setting. *Pathobiology.* 2024;91(2):114–20.
  31. Kim T, Lee A, Ahn S, Park JS, Jeun SS, Lee YS. Comprehensive molecular genetic analysis in glioma patients by next generation sequencing. *Brain Tumor Res Treat.* 2024;12(1):23–39.
  32. Tsantikidi A, Papadopoulou E, Metaxa-Mariatou V, Kapetsis G, Tsaousis G, Meintani A, et al. The utility of NGS analysis in homologous recombination deficiency tracking. *Diagnostics (Basel).* 2023;13(18):2962.

## Authors and Affiliations

Eloisa Jantus-Lewintre<sup>1</sup> · Alessandra Rappa<sup>2</sup> · Dina Ruano<sup>3</sup> · Demi van Egmond<sup>3</sup> · Sandra Gallach<sup>1</sup> · Dilce Gozuyasli<sup>4</sup> · Cecília Durães<sup>4</sup> · José Luis Costa<sup>4</sup> · Carlos Camps<sup>5</sup> · Ludovic Lacroix<sup>6</sup> · Karl Kashofer<sup>7</sup> · Tom van Wezel<sup>3,8</sup> · Massimo Barberis<sup>2</sup>

✉ Massimo Barberis  
massimo.barberis@ieo.it

<sup>1</sup> Fundació Investigación Hospital General Universitario de València, Universitat Politècnica de València, CIBERONC, Valencia, Spain

<sup>2</sup> Istituto Europeo di Oncologia, IRCCS, Via Adamello 16, 20139 Milan, Italy

<sup>3</sup> Leiden University Medical Center, Leiden, The Netherlands

<sup>4</sup> Thermo Fisher Scientific, Waltham, MA, USA

<sup>5</sup> Consorcio Hospital General Universitario de València, Universitat de València, CIBERONC, Valencia, Spain

<sup>6</sup> Institut Gustave Roussy, Paris, France

<sup>7</sup> Medical University of Graz, Graz, Austria

<sup>8</sup> Netherlands Cancer Institute, Amsterdam, The Netherlands